Biochimica et Biophysica Acta 1847 (2015) 441–450

Contents lists available at ScienceDirect

Biochimica et Biophysica Acta

journal homepage: www.elsevier.com/locate/bbabio

Redox regulation of CF_1-ATPase involves interplay between the γ-subunit neck region and the turn region of the βDELSEED-loop

Felix Buchert [a], Hiroki Konno [a,b], Toru Hisabori [a,c,*]

[a] Chemical Resources Laboratory, Tokyo Institute of Technology, Nagatsuta 4259-R1-8, Midori-ku, Yokohama 226-8503, Japan
[b] Imaging Research Division, Bio-AFM Frontier Research Center, Kanazawa University, Kakuma, Kanazawa 920-1192, Japan
[c] Core Research for Evolutional Science and Technology (CREST), Japan Science and Technology Agency (JST), Tokyo 102-0075, Japan

ARTICLE INFO

Article history:
Received 6 November 2014
Received in revised form 23 December 2014
Accepted 27 January 2015
Available online 7 February 2015

Keywords:
Chloroplast ATP synthase
ATPase redox regulation
βDELSEED-loop
Subunit interaction
Cysteine-mediated cross-linking
Thiol labeling

ABSTRACT

The soluble F_1 complex of ATP synthase (F_oF_1) is capable of ATP hydrolysis, accomplished by the minimum catalytic core subunits $\alpha_3\beta_3\gamma$. A special feature of cyanobacterial F_1 and chloroplast F_1 (CF_1) is an amino acid sequence inserted in the γ-subunit. The insertion is extended slightly into the CF_1 enzyme containing two additional cysteines for regulation of ATPase activity via thiol modulation. This molecular switch was transferred to a chimeric F_1 by inserting the cysteine-containing fragment from spinach CF_1 into a cyanobacterial γ-subunit [Y. Kim et al., redox regulation of rotation of the cyanobacterial F_1-ATPase containing thiol regulation switch, J Biol Chem, 286 (2011) 9071–9078]. Under oxidizing conditions, the obtained F_1 tends to lapse into an ADP-inhibited state, a common regulation mechanism to prevent wasteful ATP hydrolysis under unfavorable circumstances. However, the information flow between thiol modulation sites on the γ-subunit and catalytic sites on the β-subunits remains unclear. Here, we clarified a possible interplay for the CF_1-ATPase redox regulation between structural elements of the βDELSEED-loop and the γ-subunit neck region, i.e., the most convex part of the α-helical γ-termini. Critical residues were assigned on the β-subunit, which received the conformation change signal produced by disulfide/dithiol formation on the γ-subunit. Mutant response to the ATPase redox regulation ranged from lost to hypersensitive. Furthermore, mutant cross-link experiments and inversion of redox regulation indicated that the γ-redox state might modulate the subunit interface via reorientation of the βDELSEED motif region.

© 2015 Elsevier B.V. All rights reserved.

1. Introduction

ATP synthase is ubiquitously found in the energy-transducing membranes of bacteria and mitochondria as well as in the photosynthetic membranes of chloroplasts and cyanobacteria [reviewed in 1]. The enzyme consists of a soluble F_1 complex and a membrane-spanning F_o complex and is therefore referred to as F_oF_1. The F_o complex is powered by an electrochemical H^+ (or Na^+) gradient, generated by electron transfer processes, across the membrane. Functional coupling of the F_o and F_1 complexes facilitates ATP synthesis by F_1 upon H^+ translocation along the electrochemical gradient through F_o. There are substantial structural similarities between eukaryotic and bacterial enzymes. The F_o complexes from bacteria, which consist of three subunits with a stoichiometry of $a_1b_2c_{10-15}$, function as proton pumps. Bacterial F_1 complexes consist of subunits $\alpha_3\beta_3\gamma\delta\varepsilon$, although the $\alpha_3\beta_3\gamma$ complex is sufficient to perform ATP hydrolysis [2]. Ion translocation drives rotation of the c_{10-15} ring in F_o as well as the γ- and ε-subunits in F_1. Contacts are formed and disrupted alternately between the rotating γ-subunit and static β-subunits of the $\alpha_3\beta_3$ hexamer [3–6]. Thus, structural changes in the three catalytic sites, primarily located on the β-subunit, are achieved in a cooperative manner [7].

The ATPase activity of F_oF_1 is regulated by a common mechanism known as ADP inhibition [8–10]. This mechanism is effective when ATP hydrolysis is favored over ATP synthesis. Release of tightly bound MgADP from the catalytic site can be accomplished by ATP binding to non-catalytic sites on the α-subunits [11], by anions [12] or by detergents like LDAO [13,14]. More specific regulation mechanisms are found in mitochondrial F_oF_1, which possess an intrinsic inhibitor protein IF_1 [15], or in bacterial [16] and chloroplast ATPases [17], where the ε-subunit acts as an intrinsic inhibitor of ATP hydrolysis. A regulatory mechanism that is exclusively found in the chloroplast F_oF_1 is thiol modulation, also termed ATPase redox regulation. Thiol modulation is accomplished by two cysteines located in a specific sequence of approximately 40 amino acids inserted in the chloroplast F_1 (CF_1) γ-subunit [18–20]. Disulfide formation inhibits futile ATP hydrolysis.

Abbreviations: F_oF_1, F_oF_1 ATP synthase; CF_1, chloroplast F_1; TF_1, *Bacillus* PS3 F_1; $F_{1\text{-redox}}$, redox-sensitive F_1 derived from the $\alpha_3\beta_3\gamma$ complex of *Thermosynechococcus elongatus* BP-1; γMLCA, set of mutations in the $F_{1\text{-redox}}$ γ-subunit γM24L/γC90A/γM280L/γM283L; Trx-*f*, thioredoxin *f*; LDAO, N-dimethyldodecylamine-N-oxide; AMS, 4-acetamido-4′-maleimidylstilbene-2,2′-disulfonic acid; V_R/V_O, $Vmax_{reduced}/Vmax_{oxidized}$

* Corresponding author at: Chemical Resources Laboratory, Tokyo Institute of Technology, Nagatsuta 4259-R1-8, Midori-ku, Yokohama 226-8503, Japan. Tel.: +81 45 924 5234; fax: +81 45 924 5268.
E-mail address: thisabor@res.titech.ac.jp (T. Hisabori).

http://dx.doi.org/10.1016/j.bbabio.2015.01.013
0005-2728/© 2015 Elsevier B.V. All rights reserved.

This inhibition is overcome upon reduction of the γ-subunit in light, which is facilitated by the reduced form of thioredoxin [21]. However, ATP synthesis mode is not regulated by thiol modulation under standard light–dark conditions [22–24]. Cyanobacteria do not possess regulatory cysteines in their γ-subunits, although a similar γ-insertion can be found [20,25]. However, the regulation mechanism found in CF_1 was successfully transferred to a cyanobacterial enzyme by insertion of the cysteine-containing fragment from spinach CF_1 into the globular domain of the prokaryotic γ-subunit [26]. A major benefit of studying the ATPase redox regulation is the preservation of crucial interactions between the γ-stalk and the $\alpha_3\beta_3$ hexamer, despite the insertion. Subsequent single-molecule analysis of the chimeric F_1 showed that the propensity to lapse into the ADP-inhibited state is higher under oxidizing conditions. Still, little is known about molecular events that facilitate this unique ATPase regulation mechanism.

Making use of the chimeric F_1 system, the study presented here aimed to improve our understanding of the molecular mechanism of this regulatory feature, which bridges an approximate distance of 60 Å [20,27] between the thiol modulation sites on the γ-subunit and the catalytic sites on β-subunits, where ADP inhibition takes place (Fig. 1A). For this purpose, we focused on the highly conserved regions of the γ- and β-subunits, which form an interface between the γ-subunit neck region and the βDELSEED-loop (Fig. 1B). The outcome, which is discussed with respect to previous observations, allowed us to update an existing model of the ATPase redox regulation.

2. Materials and methods

2.1. Materials

Aldrithiol-2, ATP, pyruvate kinase, lactate dehydrogenase, and phosphoenolpyruvate were purchased from Sigma. NADH was purchased from Roche Diagnostics. 4-acetamido-4′-maleimidylstilbene-2,2′-disulfonic acid (AMS) was purchased from Molecular Probe. Other chemicals were of the highest grade commercially available.

2.2. Strains

Escherichia coli strain DH5α was used for cloning and strain BL21(DE3)uncΔ702 [29] was used to express the $\alpha_3\beta_3\gamma$ complex of *Thermosynechococcus elongatus* BP-1 ATPase. The latter strain was a kind gift from Dr. C. S. Harwood (University of Iowa).

2.3. Construction of expression plasmids

An expression vector for ATPase rotation studies [26] was double-digested with *Sac*I and *Nhe*I. The 464 bp fragment containing *atpC* was ligated into a *Sac*I-/*Nhe*I-digested plasmid used to express the wild-type $\alpha_3\beta_3\gamma$ obtained from *T. elongatus* BP-1, as previously described [30]. The insert contained the sequence encoding the spinach CF_1 γ-redox region. The redox regulatory cysteines were numbered as γC200 and γC206 in this study. The resulting construct was used to express a redox-sensitive chimeric F_1 $\alpha_3\beta_3\gamma$ complex referred to as $F_{1\text{-redox}}$. *Eco*RI/*Nhe*I restriction fragments and *Nhe*I/*Hind*III restriction fragments were cloned in digested vector backbones to obtain the γ- and β-subunit mutant enzymes, respectively. Abutting primers and oligonucleotides for the mega-primer method [31] (Supplementary Table 1) were used when introducing mutations.

2.4. Expression and purification of the $\alpha_3\beta_3\gamma$ complex

The methods applied here were slightly modified from previous reports [30,32]. The complex was purified from *E. coli* cell extracts in Buffer A, which contained 20 mM HEPES–KOH (pH 8.0), 100 mM KCl, 0.1 mM $MgCl_2$, 0.1 mM ADP, and 50 mM imidazole. The heat treatment step conducted prior to nickel–nitrilotriacetic acid chromatography was omitted. After gel-filtration chromatography on a Superdex 200 column (16/30, Amersham Biosciences), the complex was frozen in storage buffer (imidazole-free buffer A and 10% v/v glycerol).

2.5. Other proteins

Expression of recombinant thioredoxin *f* (Trx-*f*) of *Spinacia oleracea* in *E. coli* and purification was carried out as previously described [33].

2.6. Measurement of ATP hydrolysis activity

Activity measurements were carried out as previously described [32], except for phosphoenolpyruvate, which was used at 0.2 mM.

2.7. Cysteine modifications

Formation and cleavage of the disulfide bond between regulatory cysteines γC200 and γC206 were promoted by incubation of 1 μM F_1 with 500 μM Aldrithiol-2 and 50 mM DTT for 60 min at 37 °C, yielding oxidized and reduced complex, respectively. In some experiments,

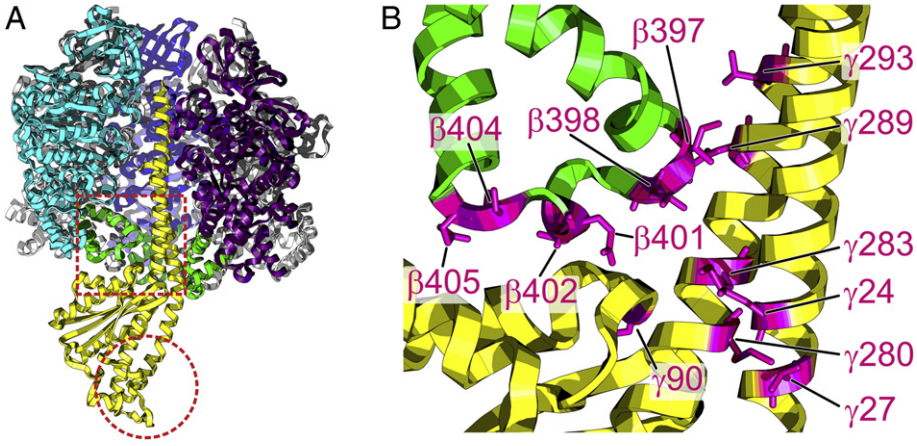

Fig. 1. Overview of the sites investigated. (A) *E. coli* F_1 $\alpha_2\beta_3\gamma$ [28, PDB: 3OAA]. One of the α-subunits (gray) was removed to allow a better depiction of the γ-subunit (yellow). Nucleotide binding states of the β-subunits (violet for empty, blue for ADP-bound, cyan for ATP-bound) as well as the βDELSEED-loop (green) were considered. The dashed circle indicates the approximate position of the inserted sequence found in cyanobacterial and CF_1 γ-subunits. (B) The magnification of the dashed square area from (A) highlights the positions and numbering of the analyzed amino acids (magenta).

recombinant spinach Trx-*f*, pre-treated with 8-fold molar excess DTT for 60 min at 25 °C, served as the reductant for the regulatory γ-cysteines. The free thiols in F_1 complexes were labeled with AMS after the F_1 was precipitated in 5% v/v trichloroacetic acid and washed with acetone. The reaction was carried out for 15 min at 25 °C in 100 mM HEPES–KOH (pH 8.0), 1% w/v SDS, and 1.1 mM AMS. The cross-linking experiments were carried out as previously reported [34], with minor modifications. F_1 (1 μM) was incubated in storage buffer containing 2 mM ATP, 2 mM $MgCl_2$, and 500 μM Aldrithiol-2 (or 0.25 μM $CuCl_2$ where indicated) for 60 min at 37 °C. Samples were treated with 10 mM N-ethylmaleimide for 10 min prior to further processing.

2.8. Protein visualization

AMS-labeled F_1 was visualized using 12% SDS-PAGE gels [35]. Other samples were analyzed using 10% gels. For labeling and cross-link experiments, 2-mercaptoethanol was omitted during SDS-PAGE. Unless otherwise stated, gels were stained with silver [36]. Western blotting was carried out as previously reported [37] using penta-histidine monoclonal antibodies from mouse (Qiagen; diluted 1:2000) and HRP-linked anti-mouse antibodies (GE Healthcare; diluted 1:10,000). Chemiluminescence was monitored using an LAS-3000 mini luminescence analyzer with IMAGE GAUGE 3.0 software (Fuji Film, Tokyo, Japan). The crystal structure of *E. coli* F_1 [28] was presented using PyMOL software [38].

3. Results

3.1. Disruption of redox regulation in $F_{1\text{-redox}}$

A previous study reported a loss of the ATPase redox regulation resulting from the mutation of conserved residues in the spinach CF_1 γ-subunit, notably several methionine residues in the terminal α-helical elements [39]. As shown in Fig. 2A, this finding was reproduced upon replacements based on sequence homology with spinach CF_1 γ-subunit, yielding $F_{1\text{-redox}}$γMLCA (γM24L/γC90A/γM280L/γM283L). Unlike the oxidized $F_{1\text{-redox}}$, the mutant did not show increased ATPase activity upon addition of reduced Trx-*f*. As represented by the slope of $\Delta A_{340\ nm}$, the ATPase activity of the mutant slightly declined after addition of Trx-*f*. Burial of residues γC200 and γC206 in $F_{1\text{-redox}}$γMLCA could be ruled out because functional thiol modulation of the regulatory γ-cysteines was visualized using AMS labeling (Fig. 2B).

3.2. Influence of the γ-subunit redox state on the position of the βDELSEED motif

It is believed that thiol modulation in the γ-redox region changes the structure of the γ-subunit [27,40]. According to a modeled structure [27], there might be a spatial separation between the γ-redox region on the one hand (Fig. 1A) and the "catch" formed by the βDELSEED-loop and the γ-subunit neck region on the other [3]. Loss of redox regulation in $F_{1\text{-redox}}$γMLCA appeared striking because the mutations were located in the neck region (Fig. 1B) and had no influence on thiol modulation (Fig. 2B). To test whether there is a structural connection between the "catch" and the γ-redox region, we followed a disulfide cross-linking approach (Fig. 3). For this purpose, one of the regulatory γ-cysteines was removed, locking the mutant in a pseudo-reduced configuration. This allowed discrimination between the reduced γ-conformation ($F_{1\text{-redox}}$γC200A) and the oxidized γ-conformation ($F_{1\text{-redox}}$) in the complex under disulfide-promoting conditions. Additionally, the βDELSEED motif was mutated (βS404C) to have a cysteine reference in the βDELSEED-loop. To avoid intrinsic cross-linking with a cysteine-containing βDELSEED motif [4], the γC90A mutation was introduced. The results (Fig. 3) clearly demonstrate that β–β cross-linking between adjacent βDELSEED motifs occurred only when the γ-subunit was locked in the pseudo-reduced state. However, cross-linking between βC404 and the remaining γC206 was not observed.

3.3. βDELSEED interactions with the γ-subunit neck region and the ATPase redox regulation in "ionic track" mutants

Reorientation of the βDELSEED motif, triggered by the γ-redox state, is a potential basis for the redox regulation of CF_1-ATPase activity. Instead of pursuing a direct interaction between the β-subunit and the γ-redox region, we focused on cross-linking efficiency in the "catch" formed by the βDELSEED-loop and the γ-subunit neck region [3]. As shown in Fig. 4, weak β–β cross-linking was observed upon γC200A mutation, which is consistent with the findings of Fig. 3. More importantly, enhanced βC402–γC283 cross-link formation was detected

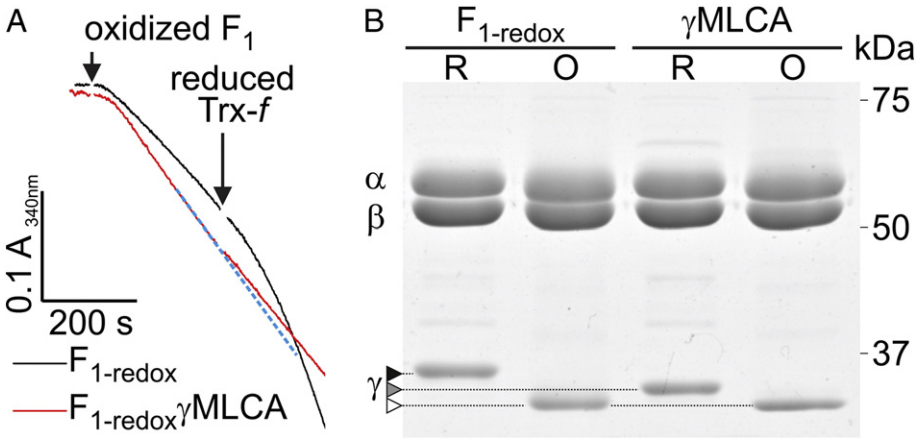

Fig. 2. Disruption of redox regulation through mutation of $F_{1\text{-redox}}$. (A) ATPase activity was assayed using an ATP-regenerating system to monitor the $A_{340\ nm}$ of NADH. Prior to assay, disulfide formation was promoted by treatment of the regulatory γ-cysteines with Aldrithiol-2. The ATPase assay was initiated by adding $F_{1\text{-redox}}$ and $F_{1\text{-redox}}$γMLCA to final concentrations of 11.3 nM and 2.3 nM, respectively. After 300 s, disulfide cleavage was promoted by addition of 5 μM reduced Trx-*f*. The blue dotted line is an extension of the $F_{1\text{-redox}}$γMLCA ATPase assay without added Trx-*f*. (B) Free thiols were visualized using SDS-PAGE and Coomassie Brilliant Blue R-250 staining. Pretreatment of 1 μM F_1 enzyme with 500 μM Aldrithiol-2 and 40 μM reduced Trx-*f* at 25 °C for 1 h yielded oxidized (O) and reduced (R) enzyme, respectively. AMS labeling was performed as described in Section 2.7. The extent of migration shift reflected the number of labeled thiols upon reduction. No γ-cysteines were labeled in the oxidized samples (white arrowhead). All 3 γ-cysteines were labeled (black arrowhead) in reduced $F_{1\text{-redox}}$. The assay of reduced $F_{1\text{-redox}}$γMLCA, which harbors γC90A, labeled only the regulatory γ-cysteine pair (gray arrowhead).

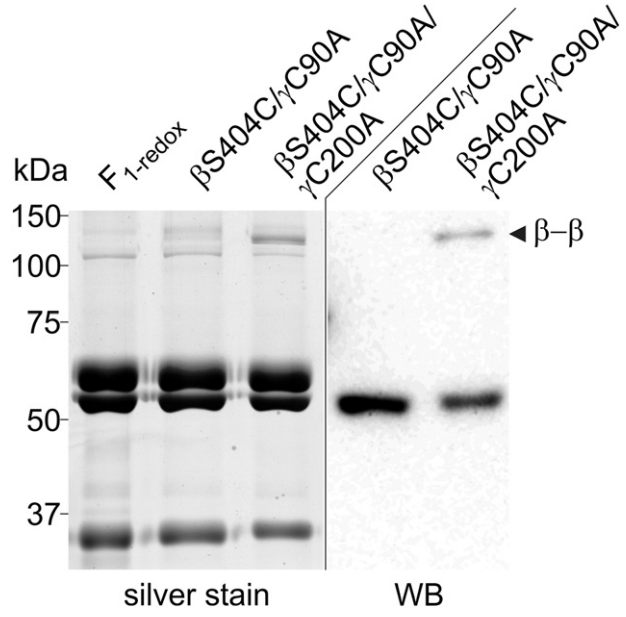

Fig. 3. Influence of the γ-subunit redox state on the position of the βDELSEED motif. Detection of β–β cross-linking in the pseudo-reduced enzyme suggests the γ-redox state-dependent rearrangement of the βDELSEED motif region. Cysteine cross-linking (arrowhead) was visualized using non-reducing SDS-PAGE followed by silver staining and western blotting (WB), as described in Sections 2.7 and 2.8. Aldrithiol-2 was used as cross-linker in the presence of MgATP.

after locking the enzyme in the pseudo-reduced conformation, indicating redox state-dependent β/γ interface adjustments between the βDELSEED-loop and the γ-subunit neck region.

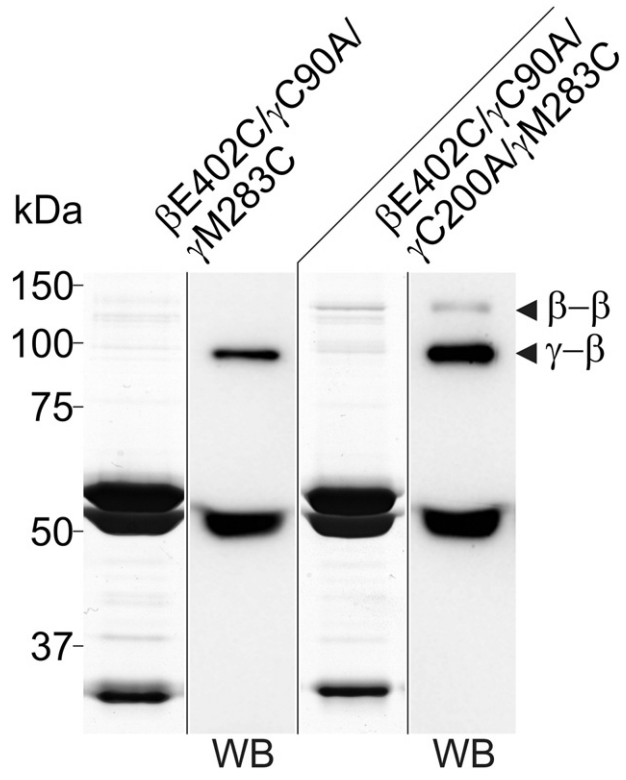

Fig. 4. βDELSEED interactions with the γ-subunit neck region. Enhanced β–γ cross-linking suggests redox state-dependent interactions between the βDELSEED motif and the γ-subunit neck region. Cysteine cross-linking (arrowhead) was visualized using non-reducing SDS-PAGE followed by silver staining and western blotting (WB) as described in Sections 2.7 and 2.8. $CuCl_2$ was used to induce a cross-link in the presence of MgATP.

The existence of an adjustable β/γ interface, termed the "ionic track" was suggested in molecular dynamic studies [41]. The "ionic track" is formed between the negatively charged cluster of residues in βDELSEED and a cluster of positively charged amino acids surrounding the γ-axis. The putative involvement of the "ionic track" in the ATPase redox regulation was investigated by measuring the activities of the oxidized and reduced $F_{1\text{-redox}}$ enzyme after single removals of charged residues from the βDELSEED motif (Fig. 5). The substitution of βE402 or βE405 had a minor impact on the activity of oxidized F_1, leaving ATP hydrolysis activities almost unchanged (Fig. 5A). Conversely, the ATPase activity of oxidized $F_{1\text{-redox}}$βD401N was approximately 3.9-fold higher than that of $F_{1\text{-redox}}$. This was probably caused by lower ADP inhibition in the mutant. Addition of the detergent LDAO minimized ADP inhibition [13,14] and stimulated the activity of oxidized $F_{1\text{-redox}}$βD401N only approximately 4.4-fold (vs. 7.7-fold in $F_{1\text{-redox}}$). The stimulation of activity by LDAO in $F_{1\text{-redox}}$βE402Q and $F_{1\text{-redox}}$βE405Q was approximately 1.7-fold and 1.1-fold higher, respectively, than in $F_{1\text{-redox}}$.

An attenuated "ionic track" in the βDELSEED mutants resulted in more sensitive ATPase redox regulation (Fig. 5B). For instance, the ATPase activity of $F_{1\text{-redox}}$ showed an approximately 2-fold activation, from 9.0 to 18.3 s^{-1}, upon reduction (Fig. 5A). $F_{1\text{-redox}}$βE405Q ATPase activation was roughly 3-fold upon reduction, i.e., from 12.5 to 36.6 s^{-1}. ATPase redox regulation effects are expressed as $Vmax_{reduced}$ / $Vmax_{oxidized} - 1$ ($V_R / V_O - 1$), yielding a value of approximately 1.0 for $F_{1\text{-redox}}$ and higher values for the βDELSEED mutants (Fig. 5B).

In the next attempt, we sought to intensify the "ionic track". By designing $F_{1\text{-redox}}$γM283R, we introduced an additional positively charged residue in the portion of the γ-subunit neck region that interacts with the βDELSEED-loop around βE402 (Fig. 4). As shown in Fig. 5C and negative $V_R / V_O - 1$ values in Fig. 5D, the putative intensification of the "ionic track" in the $F_{1\text{-redox}}$γM283R completely reversed the ATPase redox regulation. The effect was still observed when additional substitutions βD401N and βE405Q were introduced. The extent of reversed ATPase redox regulation was amplified the most in $F_{1\text{-redox}}$βE402Q/γM283R.

Taking into account the inverted effects of γM283R, the βD401N mutation increased activity the most, as observed with oxidized $F_{1\text{-redox}}$βD401N (Fig. 5A) and reduced $F_{1\text{-redox}}$βD401N/γM283R (Fig. 5C). The propensity for ADP inhibition also played a role in the modified "ionic track" mutants, as evidenced by similar LDAO stimulation ratios of oxidized $F_{1\text{-redox}}$βD401N and reduced $F_{1\text{-redox}}$βD401N/γM283R (4.4 vs. 5.0). Accordingly, a resemblance of LDAO stimulation was observed on comparing oxidized βE402Q (13.1 vs. 15.3) and βE405Q mutants (8.7 vs. 8.9) with their reduced γM283R-containing counterparts. As discussed in Section 4, stimulation of ATPase activity by LDAO was lowered when βDELSEED mutants contained the additional mutation γM283R (Fig. 5A and C). Compared with $F_{1\text{-redox}}$, ATP hydrolysis rates were not inverted by γM283R in a redox-dependent manner when LDAO was present. Taken together, these results demonstrate that adjustments of ionic interactions had a clear effect on ATPase redox regulation.

Experiments combining γM283R with the βDELSEED mutants were conducted to clarify whether inverted redox regulation was the result of a specific ionic interaction between γR283 and either βD401, βE402, or βE405. Unlike F_1 from the thermophilic *Bacillus* PS3, which served as the platform for various drastic βDELSEED mutant studies [42 and references therein], the cyanobacterial F_1 lost stability upon multiple replacements within the βDELSEED motif. Complex disassembly was demonstrated by comparing the apparent subunit ratios of purified $\alpha_3\beta_3\gamma$ using SDS-PAGE (Fig. 6A). In complexes containing multiple βDELSEED mutations, the γ-subunit was less visible, especially upon addition of γM283R. Based on this experimental restriction, it was difficult to clarify whether γR283 interacted with a particular βDELSEED residue or with the bulk of the negatively charged residues.

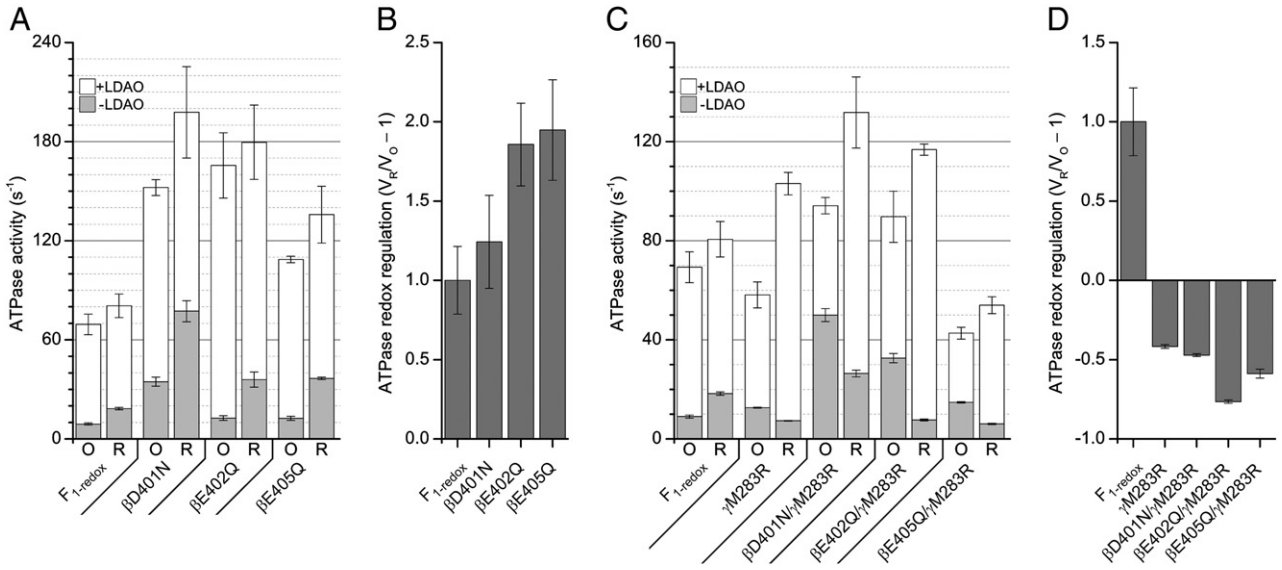

Fig. 5. Altered ATPase redox regulation in "ionic track" mutants. (A) ATP hydrolysis activities of βDELSEED motif mutants are shown. Pretreatment of F_1 enzyme with DTT and Aldrithiol-2 yielded the reduced (R) and oxidized (O) enzyme, respectively. MgATPase activity was assayed using an ATP-regenerating system for 3–5 min, followed by addition of 0.1% w/v LDAO (+LDAO) in order to overcome MgADP inhibition ($n = 3 \pm$ SD). (B) Based on the data shown in (A), the response of the mutants' ATPase to redox regulation was put into perspective by calculating $V_R / V_O - 1$. After γ-disulfide reduction, the ATPase activity of $F_{1\text{-redox}}$ was activated by a factor 2.04 which yielded $V_R / V_O - 1$ of about 1.0 ± 0.21 ($n = 3 \pm$ SD). (C) The ATPase activities of several $F_{1\text{-redox}}$γM283R mutants were assayed under the same conditions as described in (A). (D) The response of the ATPase activity to redox regulation, expressed as $V_R / V_O - 1$, was calculated using the data from (C). Redox regulation response in the mutants was reversed, yielding negative $V_R / V_O - 1$ values around −0.5.

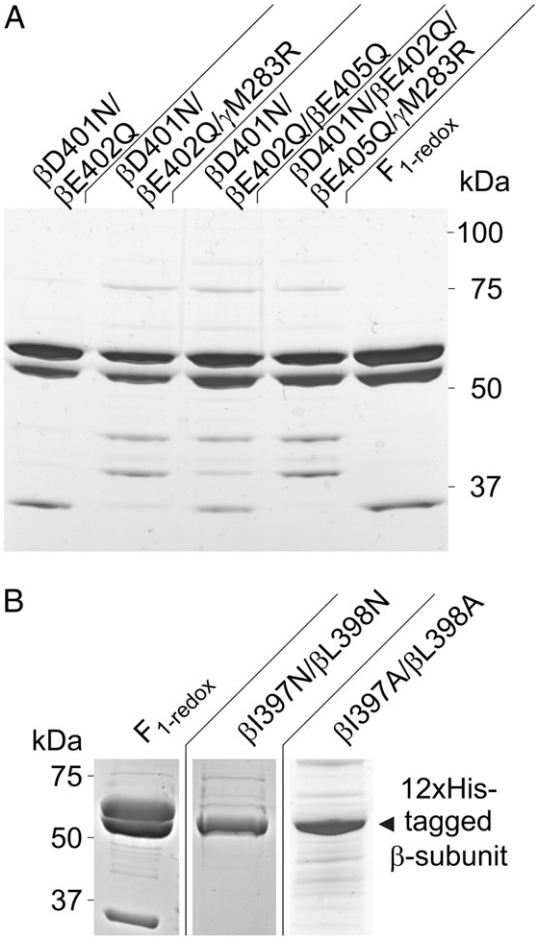

Fig. 6. Decline in $F_{1\text{-redox}}$ stability upon removal of several important amino acids. Mutants with altered properties of overall charge (A) of the βDELSEED motif, and hydrophobicity and side chain bulk (B) in the turn region of the βDELSEED-loop are shown. Results are visualized using SDS-PAGE, followed by silver staining.

3.4. Altered ATPase redox regulation by mutations in the turn region of the βDELSEED-loop

Although removing charge from the βDELSEED motif resulted in altered redox regulation properties (Fig. 5), these mutations did not disrupt the redox regulation previously observed in $F_{1\text{-redox}}$γMLCA (Fig. 2A). Recent single-molecule analyses of TF_1 revealed that drastic replacement of the whole βDELSEED motif with Ala had no effect on torque generation [42]. Moreover, these mutants contained additional N-terminal Ala substitutions in the βDELSEED-loop region, including mutations at conserved residues βI397 and βL398 (*T. elongatus* BP-1 F_1 numbering). These two residues were part of a hydrophobic turn and were also suggested to form critical hydrophobic contacts with the γ-subunit [43] which prompted us to investigate the ATPase redox regulation behavior of βI397 and βL398 mutants.

Similar to the stability loss in certain βDELSEED motif mutants mentioned in Section 3.3, our $F_{1\text{-redox}}$ complex could not be purified when βI397 and βL398 were substituted with Ala and Asn, respectively (Fig. 6B). Therefore, Val and Phe, which have a certain threshold volume [44], were chosen as appropriate hydrophobic replacements (Fig. 7). As observed with $F_{1\text{-redox}}$γMLCA (Fig. 2A and B), double mutants of the βDELSEED-loop turn region showed disrupted ATPase redox regulation, whereas disulfide/dithiol formation within the cysteines on the γ-subunit was still functional (Fig. 7). Mutants with small substituted residues showed high ATPase activity ($F_{1\text{-redox}}$βI397V/βL398V), whereas those with bulky replacements inhibited ATP hydrolysis in both γ-redox states ($F_{1\text{-redox}}$βI397F/βL398F). As revealed by LDAO stimulation of the ATPase, mutant-specific tendencies to drop into ADP inhibition were the reason for the variation in activity observed (e.g., no vs. 7.8-fold activation for oxidized $F_{1\text{-redox}}$βI397V/βL398V and $F_{1\text{-redox}}$βI397F/βL398F, respectively). Single mutations of the turn residues had various effects. In the absence of LDAO, the βL398V mutation had no consequences on ATPase activity and redox regulation. The same was true for βI397V, under oxidizing conditions. However, $F_{1\text{-redox}}$βI397V was significantly more activated upon γ-disulfide cleavage. Insertion of the bulky residue Phe at position 397 had a negative effect on activity that was overcome by addition of LDAO (e.g., 32-fold stimulation in oxidized $F_{1\text{-redox}}$βI397F). Reversed redox regulation was also observed in that

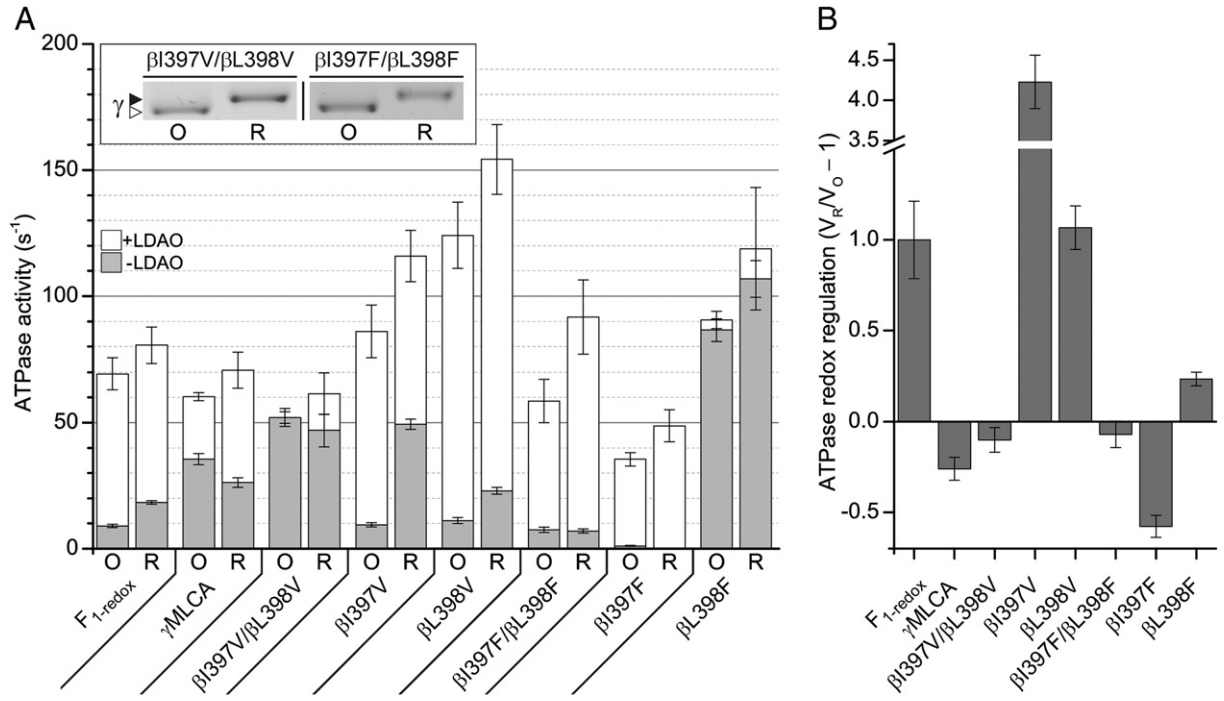

Fig. 7. ATPase redox regulation is altered by mutations in the turn region of the βDELSEED-loop. (A) ATP hydrolysis activity ($n = 3 \pm$ SD) is shown after treating samples as described in Fig. 5A. The inset visualizes representative AMS labeling of free thiols, as described in Section 2.7. Oxidized (white arrowhead) and reduced (black arrowhead) γ-subunits are highlighted. (B) The response of the ATPase activity to redox regulation was calculated using the data from (A). For a detailed description see Fig. 5B. $V_R / V_O - 1$ values above 1.0 reflected hypersensitive ATPase redox regulation response. $V_R / V_O - 1$ values around −0.5 corresponded to an inverted response, and values around 0 reflected insensitivity to ATPase redox regulation.

mutant. The mutant $F_{1\text{-redox}}$βL398F was highly active and displayed almost no response to LDAO or thiol modulation. While the activity of $F_{1\text{-redox}}$βL398V ATPase was similar to that of $F_{1\text{-redox}}$ without detergent, its activity was much higher in the presence of LDAO.

3.5. Defining the redox regulation interface in the γ-subunit neck region

A previous molecular dynamics study suggested the existence of torque-generating "hot spot" clusters formed by the hydrophobic turn (i.e., βI397 and βL398 according to *T. elongatus* BP-1 F_1 numbering) and the γ-subunit neck region [43]. Mutation-induced disturbances within these suggested clusters caused disruption of ATPase redox regulation, as shown in Section 3.4, for the hydrophobic turn of the βDELSEED-loop (Fig. 7). Regarding the γ-neck region, $F_{1\text{-redox}}$γMLCA contains mutations in all three suggested "hot spot" clusters, whereas methionine substitutions in the helical γ-termini disrupted the ATPase redox regulation most effectively [39]. In order to define the involvement of the β/γ interface in redox regulation in more detail, cysteines were introduced along the C-terminal α-helix of the γ-subunit, and at position 397 in the β-subunit (Fig. 8A and Supplementary Fig. 1). In addition, the enzyme was locked in the pseudo-reduced conformation by the γC200A mutation, so that relative movements of the βDELSEED-loop around βC397 could be investigated depending on the γ-redox state. Analysis of β–γ disulfide cross-linking revealed

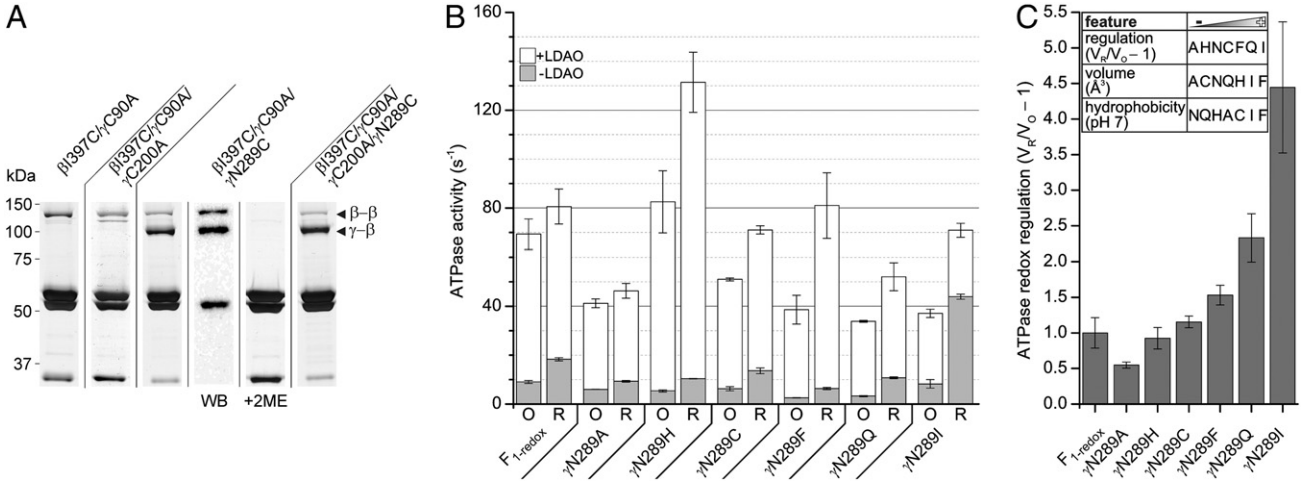

Fig. 8. Defining the redox regulatory β/γ interface in the γ-subunit C-terminus. (A) Cysteine cross-linking (arrowhead) was visualized using non-reducing SDS-PAGE followed by silver staining and western blotting (WB), as described in Sections 2.7 and 2.8. Aldrithiol-2 was used as a cross-linker in the presence of MgATP. Where indicated, 2-mercaptoethanol in the sample buffer (+2ME) cleaved the disulfide cross-links. (B) ATP hydrolysis activity ($n = 3 \pm$ SD) is shown after treating samples as described in Fig. 5A. (C) The response of the ATPase activity to redox regulation was calculated using the data from (B). For details see Fig. 5B. The inset orders γ-residues analyzed at position 289 according to their increasing response of the ATPase redox regulation, their increasing volume [44], and their increasing hydrophobicity [45].

that βC397/γC289 contacts were formed in both oxidized and pseudo-reduced F_1 (Fig. 8A). On the other hand, no βC397–γC283 cross-linking was detected in either γ-redox state, although weak βC397–γC293 cross-link formation was observed (Supplementary Fig. 1). The β–γ disulfide cross-link approach did not provide evidence for γC200A-induced large-scale movement of the βDELSEED-loop around βC397 with respect to the γ-subunit C-terminal axis. In agreement with a previous study [34], the βI397C replacement resulted in β–β cross-linking in all mutants tested. Based on the results displayed in Fig. 8A, a series of γN289 mutants were analyzed for the ATPase redox regulation behavior (Fig. 8B). Replacement of γN289 resulted in various effects, ranging from slightly weakened to substantially enhanced redox regulation sensitivity, whereas none of the analyzed mutations truly abolished or inverted redox regulation (Fig. 8C). The response to redox regulation upon γN289 replacement did not appear to be associated with the volume [44] or hydrophobicity [45] of the substituent, whereas the three bulkiest replacements (Fig. 8C) showed the largest difference between oxidized and reduced LDAO-stimulated ATPase (Fig. 8B).

A similar cross-link approach served to define the redox regulation interface between βC397 and the γ-subunit N-terminus. Again, β–γ disulfide cross-linking was detected in a γ-redox state-independent manner (Fig. 9A). Mutations γM24C and γV27C promoted weak and significant β–γ cross-linking, respectively. ATPase redox regulation mutants showed diverse effects (Fig. 9B and C). The conservative γM24I mutation resulted in no change in redox regulation. However, ADP inhibition was lowered due to enhanced basal levels of ATPase activity and weakened LDAO stimulation. $F_{1\text{-redox}}$γM24V showed more sensitive redox regulation with enhanced basal activity in the oxidized state and abolished LDAO stimulation in the reduced state. Previously, a homologous substitution of $F_{1\text{-redox}}$γM24L was shown to abolish redox regulation [39] which confirms the sensitivity of that particular γ-region. Similarly, $F_{1\text{-redox}}$γV27A showed disrupted redox regulation accompanied by enhanced ATPase activity in the absence and the presence of LDAO (Fig. 9B and C). An analysis of the redox regulation of the ATPase activities of mutants is presented in Table 1.

Table 1
Overview of the ATPase redox regulation observed in $F_{1\text{-redox}}$ mutants.

$F_{1\text{-redox}}$ mutant enzyme	Effect on ATPase redox regulation
Ionic interactions between the βDELSEED motif and the γ-subunit	
βD401N	Slightly enhanced
βE402Q	Enhanced
βE405Q	Enhanced
γM283R	Reversed
Steric/hydrophobic interactions between the βI397–βL398 turn and the γ-subunit	
βI397/βL398 double mutants	Lost
βI397V/βI397F	Strongly enhanced/reversed
βL398V/βL398F	No effect/impaired
Interactions between the γ-subunit and the βDELSEED-loop	
γM24V/γM24I	Enhanced/no effect
γV27A	Impaired
γN289 mutations	Manifold

4. Discussion

Unlike their mitochondrial or bacterial counterparts, crystal structures of the cyanobacterial and CF_1 $\alpha_3\beta_3\gamma$ are not currently available. These limitations, particularly the lack of an available CF_1 γ-subunit structure, narrow the range of study designs available to functionally analyze the unique mechanism of redox regulation. Nevertheless, several conclusions can be drawn based on the existence of the 30–40 amino acid insertions found in CF_1 γ-subunits and their progenitors. Early studies linked structural rearrangements in the CF_1 γ-subunit to thylakoid membrane energization [46–50] and thiol modulation [51]. More recently, a structural model was proposed that incorporates an open conformation upon γ-dithiol formation and a compact conformation upon γ-disulfide formation [27]. In addition, single-molecule experiments using the cyanobacterial enzyme concluded that the propensity for ADP inhibition can be attributed to the insert, which is also found in CF_1 γ-subunits [52] and that the probability of F_1 to lapse into an ADP-inhibited state, which results in a lower ATPase activity, is higher when a γ-disulfide is formed [26,

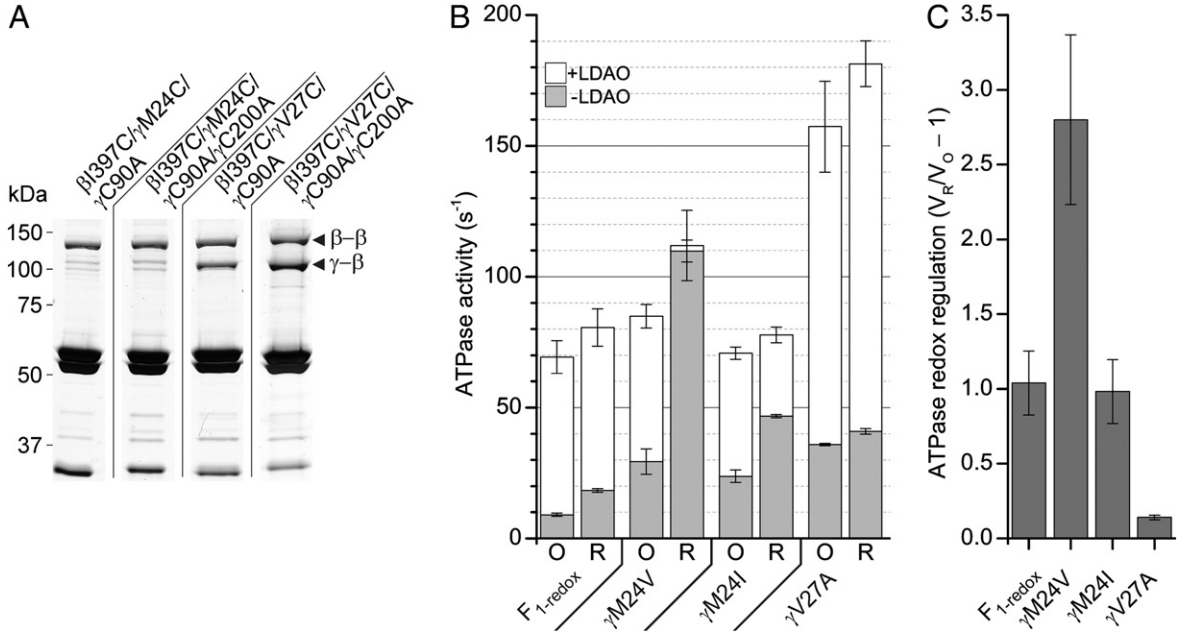

Fig. 9. Defining the redox regulation β/γ interface in the γ-subunit N-terminus. (A) Cysteine cross-linking (arrowhead) was visualized using non-reducing SDS-PAGE followed by silver staining, as described in Section 2.7. Aldrithiol-2 was used as a cross-linker in the presence of MgATP. (B) ATP hydrolysis activity ($n = 3 \pm$ SD) is shown after treating samples as described in Fig. 5A. (C) The response of the ATPase activity to redox regulation was calculated using the data from (B). For details see Fig. 5B.

53]. Despite these advances, the mechanism through which the γ-cysteine redox switch influences the nucleotide binding behavior of the β-subunit is not yet understood.

This study elaborated on the functional connection between information produced by γ-disulfide formation/cleavage and the β-subunit, acting as a recipient of this information. Most of the mutants differed in their ATPase activities which was most likely the result of altered intra-/inter-subunit interactions. Accordingly, (I) ionic, (II) van der Waals, (III) redox-specific, and (IV) hydrophobic interactions, as well as (V) other aspects will be considered as potential causes for mutant ATPase rates and redox regulation. In general, ATPase activity is determined by factors such as ATP binding to non-catalytic sites, cooperativity between catalytic sites, and MgADP inhibition. ADP inhibition could be overcome by adding LDAO [13,14], which indicated whether inhibition properties were changed in the mutants.

(I) LDAO also enhances the efficiency of subunit cooperativity in *E. coli* F_1 [14], which might be relevant for the LDAO-stimulated ATPase of attenuated and intensified "ionic track" mutants in Fig. 5. Changing the sum of ionic interactions between the βDELSEED motif and the γ-subunit neck might influence the impact of LDAO on subunit cooperativity.

(II) ADP inhibition properties, and therefore ATPase activities, might also be influenced by the van der Waals volumes of the amino acid side chains in the turn region of the βDELSEED-loop (Fig. 7). Bulky amino acid side chains resulted in a higher propensity toward ADP inhibition and thus lower ATPase activity. Modulated side chain bulk might result in diverged ATPase activity, even after overcoming ADP inhibition.

(III) Relocation events in the β-subunit that depended on the redox state of the γ-subunit might increase the sum of the interactions in the oxidized $F_{1\text{-redox}}$ enzyme, which were partly canceled by the addition of LDAO. Hence the gap in ATPase activity between the oxidized and reduced forms in the presence of LDAO might be widened in bulky γN289 mutants (Fig. 8). Even mutants with reversed redox regulation showed that trend once LDAO was added (Fig. 5C), suggesting that restrictive charge interactions of a mutated "ionic track" were overcome by LDAO, while redox-specific steric constraints prevailed.

(IV) Some data disagreed with γ-redox state-triggered van der Waals contacts: Although steric clashes were supposed to be more likely, $F_{1\text{-redox}}$βL398F was highly active and its redox regulation was impaired (Fig. 7). Instead, the ATPase activity upon introduction of βL398F might be the result of altered hydrophobic properties of the β/γ interface, which could lead to complex instability in other cases (Fig. 6B).

(V) On the other hand, conclusions based on hydrophobicity did not always apply, as exemplified by $F_{1\text{-redox}}$γN289Q, which had $F_{1\text{-redox}}$-like hydrophobic properties [45] but low ATPase activity in the presence of LDAO, as seen in Fig. 8. Inconsistencies could be attributed to unpredictable α-helical properties of the mutated γ-termini. It could be that relevant interactions were altered in the vicinity of the actual substitution sites. As seen for γM24 (Fig. 9), an interaction with βI397 was not required for changed ADP inhibition and redox regulation upon mutation. Some contradictions in our study might be attributed to an additional parameter that was described recently and could play a role in the CF_1-ATPase redox regulation in general [32]. Therein, the authors demonstrated that restricting relative slippage of the γ-termini diminishes ADP inhibition.

The cartoon model in Fig. 10 summarizes our findings and is consistent with previous suggestions about how the redox regulation mechanism might work [26,32]. During ATPase redox regulation, movements of the γ-termini could be restrictively modulated in reduced CF_1 and thus lower ADP inhibition. Triggered by γ-disulfide cleavage, the adjustment of the γ-termini movements could be accomplished by the β-subunit after relocation of the βDELSEED motif region. The hydrophobic turn of the βDELSEED-loop could act as a γ-redox state-dependent claw that controls the relative slippage behavior of the γ-termini and thus, the ATP hydrolysis activity.

5. Conclusions

The results of this study provide evidence for wide-ranging structural rearrangements in an F_1 enzyme upon γ-disulfide formation/cleavage. The ATPase redox switch involves ionic, hydrophobic, and van der Waals interactions that are most likely reassigned in a sophisticated manner. The redox regulation interface is formed by the βDELSEED-loop, in particular the hydrophobic turn, and the γ-subunit neck region. Based on our investigations, further single-molecule experiments and cross-linking studies might provide additional insights into how the ATPase redox regulation affects torque generation and the degree of

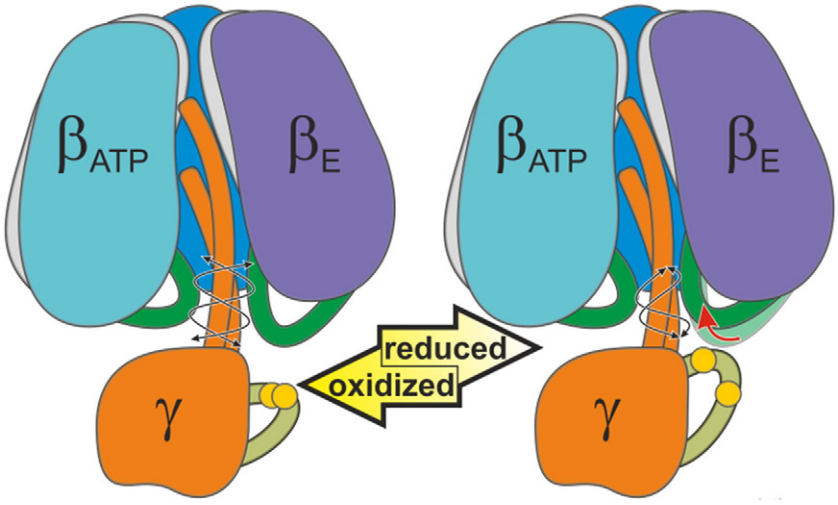

Fig. 10. Model of ATPase redox regulation. Interaction of the CF_1 γ-subunit (orange) with the β-subunit (color code as in Fig. 1A; β_E and β_{ATP} refer to the empty and ATP-bound states, respectively). Reduction of regulatory cysteines (yellow balls) generates steric repulsion between the extended 40 amino acid γ-insertion (olive) and the βDELSEED-loop (green). Consequently, reorientation (red arrow) of the βDELSEED-loop modulates the interface with the γ-subunit neck region and relative slippage of the helical γ-termini (black twisted double arrows) are restricted, resulting in elevated ATPase due to lowered ADP inhibition efficiency.

relative γ-termini movements. A previous charge removal approach close to the regulatory γ-cysteines also resulted in reversed ATPase redox regulation [54]. Regarding the putative reorientation of the βDELSEED motif, artificial ionic interactions might help to clarify the yet unknown subunit rearrangements during ATPase redox regulation.

Transparency document

The Transparency document associated with this article can be found, in the online version.

Acknowledgements

This work was supported in part by a Postdoctoral Fellowship for Foreign Researchers (P12389 to F.B.) from the Japan Society for the Promotion of Science and the Core Research of Evolutional Science and Technology program (CREST) from the Japan Science and Technology Agency (JST) (to T. H.).

Appendix A. Supplementary data

Supplementary data to this article can be found online at http://dx.doi.org/10.1016/j.bbabio.2015.01.013.

References

[1] T. Hisabori, E.I. Sunamura, Y. Kim, H. Konno, The chloroplast ATP synthase features the characteristic redox regulation machinery, Antioxid. Redox Signal. 19 (2013) 1846–1854.
[2] T. Matsui, M. Yoshida, Expression of the wild-type and the Cys-/Trp-less $\alpha_3\beta_3\gamma$ complex of thermophilic F_1-ATPase in *Escherichia coli*, Biochim. Biophys. Acta Bioenerg. 1231 (1995) 139–146.
[3] J.P. Abrahams, A.G. Leslie, R. Lutter, J.E. Walker, Structure at 2.8 Å resolution of F_1-ATPase from bovine heart mitochondria, Nature 370 (1994) 621–628.
[4] T.M. Duncan, V.V. Bulygin, Y. Zhou, M.L. Hutcheon, R.L. Cross, Rotation of subunits during catalysis by *Escherichia coli* F_1-ATPase, Proc. Natl. Acad. Sci. U. S. A. 92 (1995) 10964–10968.
[5] D. Sabbert, S. Engelbrecht, W. Junge, Intersubunit rotation in active F-ATPase, Nature 381 (1996) 623–625.
[6] H. Noji, R. Yasuda, M. Yoshida, K. Kinosita Jr., Direct observation of the rotation of F_1-ATPase, Nature 386 (1997) 299–302.
[7] M.J. Gresser, J.A. Myers, P.D. Boyer, Catalytic site cooperativity of beef heart mitochondrial F_1 adenosine triphosphatase. Correlations of initial velocity, bound intermediate, and oxygen exchange measurements with an alternating three-site model, J. Biol. Chem. 257 (1982) 2030–2038.
[8] I.B. Minkov, A.F. Fitin, E.A. Vasilyeva, A.D. Vinogradov, Mg^{2+}-induced ADP-dependent inhibition of the ATPase activity of beef heart mitochondrial coupling factor F_1, Biochem. Biophys. Res. Commun. 89 (1979) 1300–1306.
[9] K.R. Dunham, B.R. Selman, Regulation of spinach chloroplast coupling factor 1 ATPase activity, J. Biol. Chem. 256 (1981) 212–218.
[10] E.A. Vasilyeva, I.B. Minkov, A.F. Fitin, A.D. Vinogradov, Kinetic mechanism of mitochondrial adenosine triphosphatase. ADP-specific inhibition as revealed by the steady-state kinetics, Biochem. J. 202 (1982) 9–14.
[11] T. Matsui, E. Muneyuki, M. Honda, W.S. Allison, C. Dou, M. Yoshida, Catalytic activity of the $\alpha_3\beta_3\gamma$ complex of F_1-ATPase without noncatalytic nucleotide binding site, J. Biol. Chem. 272 (1997) 8215–8221.
[12] Z.Y. Du, P.D. Boyer, On the mechanism of sulfite activation of chloroplast thylakoid ATPase and the relation of ADP tightly bound at a catalytic site to the binding change mechanism, Biochemistry 29 (1990) 402–407.
[13] J.M. Jault, C. Dou, N.B. Grodsky, T. Matsui, M. Yoshida, W.S. Allison, The $\alpha_3\beta_3\gamma$ subcomplex of the F_1-ATPase from the thermophilic *Bacillus* PS3 with the βT165S substitution does not entrap inhibitory MgADP in a catalytic site during turnover, J. Biol. Chem. 271 (1996) 28818–28824.
[14] S.D. Dunn, R.G. Tozer, V.D. Zadorozny, Activation of *Escherichia coli* F_1-ATPase by lauryldimethylamine oxide and ethylene glycol: relationship of ATPase activity to the interaction of the ε and β subunits, Biochemistry 29 (1990) 4335–4340.
[15] E. Cabezon, I. Arechaga, P. Jonathan, G. Butler, J.E. Walker, Dimerization of bovine F_1-ATPase by binding the inhibitor protein, IF_1, J. Biol. Chem. 275 (2000) 28353–28355.
[16] J. Weber, S.D. Dunn, A.E. Senior, Effect of the ε-subunit on nucleotide binding to *Escherichia coli* F_1-ATPase catalytic sites, J. Biol. Chem. 274 (1999) 19124–19128.
[17] M.L. Richter, W.J. Patrie, R.E. McCarty, Preparation of the ε subunit and ε subunit-deficient chloroplast coupling factor-1 in reconstitutively active forms, J. Biol. Chem. 259 (1984) 7371–7373.
[18] C.M. Nalin, R.E. McCarty, Role of a disulfide bond in the γ subunit in activation of the ATPase of chloroplast coupling factor-1, J. Biol. Chem. 259 (1984) 7275–7280.
[19] J. Miki, M. Maeda, Y. Mukohata, M. Futai, The γ subunit of ATP synthase from spinach chloroplasts — primary structure deduced from the cloned cDNA sequence, FEBS Lett. 232 (1988) 221–226.
[20] T. Hisabori, H. Ueoka-Nakanishi, H. Konno, F. Koyama, Molecular evolution of the modulator of chloroplast ATP synthase: origin of the conformational change dependent regulation, FEBS Lett. 545 (2003) 71–75.
[21] J.D. Mills, P. Mitchell, P. Schurmann, Modulation of coupling factor ATPase activity in intact chloroplasts — the role of the thioredoxin system, FEBS Lett. 112 (1980) 173–177.
[22] U. Junesch, P. Graber, Influence of the redox state and the activation of the chloroplast ATP synthase on proton-transport-coupled ATP synthesis hydrolysis, Biochim. Biophys. Acta 893 (1987) 275–288.
[23] S. Ponomarenko, I. Volfson, H. Strotmann, Proton gradient-induced changes of the interaction between CF_O and CF_1 related to activation of the chloroplast ATP synthase, FEBS Lett. 443 (1999) 136–138.
[24] H. Konno, T. Nakane, M. Yoshida, H. Ueoka-Nakanishi, S. Hara, T. Hisabori, Thiol modulation of the chloroplast ATP synthase is dependent on the energization of thylakoid membranes, Plant Cell Physiol. 53 (2012) 626–634.
[25] S. Wernergrune, D. Gunkel, J. Schumann, H. Strotmann, Insertion of a 'chloroplast-like' regulatory segment responsible for thiol modulation into γ-subunit of F_OF_1-ATPase of the cyanobacterium *Synechocystis* 6803 by mutagenesis of *atpC*, Mol. Gen. Genet. 244 (1994) 144–150.
[26] Y. Kim, H. Konno, Y. Sugano, T. Hisabori, Redox regulation of rotation of the cyanobacterial F_1-ATPase containing thiol regulation switch, J. Biol. Chem. 286 (2011) 9071–9078.
[27] M.L. Richter, H.S. Samra, F. He, A.J. Giessel, K.K. Kuczera, Coupling proton movement to ATP synthesis in the chloroplast ATP synthase, J. Bioenerg. Biomembr. 37 (2005) 467–473.
[28] G. Cingolani, T.M. Duncan, Structure of the ATP synthase catalytic complex F_1 from *Escherichia coli* in an autoinhibited conformation, Nat. Struct. Mol. Biol. 18 (2011) 701–707.
[29] N.N. Nichols, C.S. Harwood, PcaK, a high-affinity permease for the aromatic compounds 4-hydroxybenzoate and protocatechuate from *Pseudomonas putida*, J. Bacteriol. 179 (1997) 5056–5061.
[30] H. Konno, T. Murakami-Fuse, F. Fujii, F. Koyama, H. Ueoka-Nakanishi, C.G. Pack, M. Kinjo, T. Hisabori, The regulator of the F_1 motor: inhibition of rotation of cyanobacterial F_1-ATPase by the ε subunit, EMBO J. 25 (2006) 4596–4604.
[31] O. Landt, H.P. Grunert, U. Hahn, A general method for rapid site-directed mutagenesis using the polymerase chain reaction, Gene 96 (1990) 125–128.
[32] E.I. Sunamura, H. Konno, M. Imashimizu, M. Mochimaru, T. Hisabori, A conformational change of the γ subunit indirectly regulates the activity of cyanobacterial F_1-ATPase, J. Biol. Chem. 287 (2012) 38695–38704.
[33] K. Motohashi, T. Hisabori, HCF164 receives reducing equivalents from stromal thioredoxin across the thylakoid membrane and mediates reduction of target proteins in the thylakoid lumen, J. Biol. Chem. 281 (2006) 35039–35047.
[34] S.P. Tsunoda, E. Muneyuki, T. Amano, M. Yoshida, H. Noji, Cross-linking of two β subunits in the closed conformation in F_1-ATPase, J. Biol. Chem. 274 (1999) 5701–5706.
[35] H. Schagger, G. von Jagow, Tricine–sodium dodecyl sulfate-polyacrylamide gel electrophoresis for the separation of proteins in the range from 1 to 100 kDa, Anal. Biochem. 166 (1987) 368–379.
[36] M.V. Nesterenko, M. Tilley, S.J. Upton, A simple modification of Blum's silver stain method allows for 30 minute detection of proteins in polyacrylamide gels, J. Biochem. Biophys. Methods 28 (1994) 239–242.
[37] H. Towbin, T. Staehelin, J. Gordon, Electrophoretic transfer of proteins from polyacrylamide gels to nitrocellulose sheets — procedure and some applications, Proc. Natl. Acad. Sci. U. S. A. 76 (1979) 4350–4354.
[38] W.L. DeLano, J.W. Lam, PyMOL: a communications tool for computational models, Abstr. Pap. Am. Chem. Soc. 230 (2005) U1371–U1372.
[39] F. Buchert, Y. Schober, A. Römpp, M.L. Richter, C. Forreiter, Reactive oxygen species affect ATP hydrolysis by targeting a highly conserved amino acid cluster in the thylakoid ATP synthase γ subunit, Biochim. Biophys. Acta Bioenerg. 1817 (2012) 2038–2048.
[40] M.L. Richter, γ–ε interactions regulate the chloroplast ATP synthase, Photosynth. Res. 79 (2004) 319–329.
[41] J.P. Ma, T.C. Flynn, Q. Cui, A.G.W. Leslie, J.E. Walker, M. Karplus, A dynamic analysis of the rotation mechanism for conformational change in F_1-ATPase, Structure 10 (2002) 921–931.
[42] M. Tanigawara, K.V. Tabata, Y. Ito, J. Ito, R. Watanabe, H. Ueno, M. Ikeguchi, H. Noji, Role of the DELSEED loop in torque transmission of F_1-ATPase, Biophys. J. 103 (2012) 970–978.
[43] J.Z. Pu, M. Karplus, How subunit coupling produces the γ subunit rotary motion in F-1-ATPase, Proc. Natl. Acad. Sci. U. S. A. 105 (2008) 1192–1197.
[44] Y. Harpaz, M. Gerstein, C. Chothia, Volume changes on protein-folding, Structure 2 (1994) 641–649.
[45] O.D. Monera, T.J. Sereda, N.E. Zhou, C.M. Kay, R.S. Hodges, Relationship of sidechain hydrophobicity and α-helical propensity on the stability of the single-stranded amphipathic α-helix, J. Pept. Sci. 1 (1995) 319–329.
[46] R.E. McCarty, J. Fagan, Light-stimulated incorporation of N-ethylmaleimide into coupling factor-1 in spinach chloroplasts, Biochemistry 12 (1973) 1503–1507.
[47] J.V. Moroney, R.E. McCarty, Effect of proteolytic digestion on the Ca^{2+}-ATPase activity and subunits of latent and thiol-activated chloroplast coupling factor-1, J. Biol. Chem. 257 (1982) 5910–5914.
[48] W. Junge, The critical electric potential difference for photophosphorylation. Its relation to the chemiosmotic hypothesis and to the triggering requirements of the ATPase system, Eur. J. Biochem. 14 (1970) 582–592.

[49] T. Bakker-Grunwald, K. van Dam, On the mechanism of activation of the ATPase in chloroplasts, Biochim. Biophys. Acta 347 (1974) 290–298.
[50] S.R. Ketcham, J.W. Davenport, K. Warncke, R.E. McCarty, Role of the γ subunit of chloroplast coupling factor-1 in the light-dependent activation of photophosphorylation and ATPase activity by dithiothreitol, J. Biol. Chem. 259 (1984) 7286–7293.
[51] J. Schumann, M.L. Richter, R.E. McCarty, Partial proteolysis as a probe of the conformation of the γ subunit in activated soluble and membrane-bound chloroplast coupling factor-1, J. Biol. Chem. 260 (1985) 11817–11823.
[52] E.I. Sunamura, H. Konno, M. Imashimizu-Kobayashi, Y. Sugano, T. Hisabori, Physiological impact of intrinsic ADP inhibition of cyanobacterial FoF1 conferred by the inherent sequence inserted into the γ subunit, Plant Cell Physiol. 51 (2010) 855–865.
[53] D. Bald, H. Noji, M. Yoshida, Y. Hirono-Hara, T. Hisabori, Redox regulation of the rotation of F_1-ATP synthase, J. Biol. Chem. 276 (2001) 39505–39507.
[54] H. Konno, M. Yodogawa, M.T. Stumpp, P. Kroth, H. Strotmann, K. Motohashi, T. Amano, T. Hisabori, Inverse regulation of F_1-ATPase activity by a mutation at the regulatory region on the γ subunit of chloroplast ATP synthase, Biochem. J. 352 (Pt 3) (2000) 783–788.